A Hybrid Thinning Algorithm for 3D Medical Images

Kálmán Palágyi and Attila Kuba

Department of Applied Informatics, József Attila University, Szeged, Hungary

Thinning is a frequently used method for extracting skeletons in discrete spaces. This paper presents an efficient parallel algorithm for thinning elongated 3D binary objects (e.g., bony structures, vessel trees, or airway trees). The proposed algorithm directly extracts medial lines as shape features from 3D binary objects by applying a brand–new class of thinning strategy called hybrid method. Our topology preserving algorithm makes easy implementation possible and gives satisfactory results for synthetic data tests and for MR angiography brain studies.

Keywords: thinning algorithms; 3D discrete topology; preserving topology; medical image processing.

Introduction

Skeletonization provides shape features that are extracted from binary image data. It is a common preprocessing operation in raster–to–vector conversion or in pattern recognition. Its goal is to reduce the volume of elongated objects to their skeletons. In the 3D Euclidean space, the skeleton of an object is the locus of the centers of all maximal inscribed spheres (Blum, 1967). In discrete spaces, the thinning procedure is a frequently used method for generating an approximation to the continuous skeleton in a topology preserving way (Kong & Rosenfeld, 1989). Thinning is similar to peeling an onion. One step of the iterative method removes the outmost layer of an object and the entire process is repeated until only the "skeleton" is left.

There are two major methods of shape representation. The first method describes the boundary that surrounds an object. The second one gives a representation of the region that is occupied by the object to be analyzed. Boundary–based

techniques are widely used but there are some deficiencies which limit their usefulness in practical applications especially in 3D (Székely, 1996):

- methods of differential geometry are rather sensitive to noise;
- occlusion may seriously disturb boundary–based descriptors;
- they are not appropriate to catch global shape features and to make them explicit;
- they can rather poorly reveal the hierarchical organization of the shape.

The concept of skeletonization should be able to help exactly at the points listed above. The local object symmetries represented by the skeleton certainly cannot replace boundary–based shape descriptors, but they complement and support them.

The importance of the skeleton as a region–based shape feature shows an upward tendency. Some important applications have appeared in medical image processing, too. Van den Elsen et al. (1992) extracted ridge–like features in their medical image registration method. They used 3D thinning to eliminate unwanted thick ridges and blobs. Various authors built distance maps from the extracted features in their registration methods (Borgefors, 1988; Jiang et al., 1992). More accurate matching based on distance transformations can be reached if thinned feature data set is used. Thinning provides relevant information and reduces the feature search space of the geometric model to be evaluated. Gerig et al. (1993) used 3D thinning for symbolic description of cerebral vessel tree. Székely et al. (1995) applied a 3D thinning algorithm in structural description of cerebral
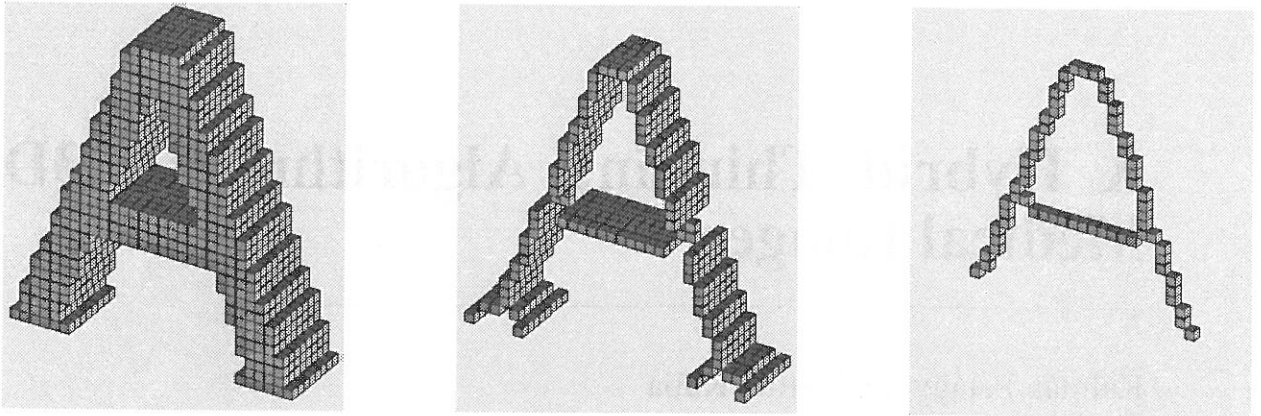
Fig. 1. A 3D synthetic picture containing a character "A" (left); its medial surface (centre); its medial lines (right). A point of a 3D binary picture can be modelled by a lattice point or by a unit cube. In this figure cubes represent black points.

vascularity. Ma & Sonka (1996) developed a 3D algorithm for thinning airway trees extracted from 3D CT studies. Näf et al. (1997) proposed skeletons for the characterization and recognition of 3D organ shape. A method has been published by Tari et al. (1997) for extracting shape skeletons from medical images.

In this paper, a new 3D thinning algorithm is proposed which directly extracts medial lines (consisting of arcs and/or curves instead of surfaces). Each iteration step contains 10 successive subiterations. Subiterations can be executed in parallel. It means that the object elements that satisfy the actual deletion conditions are to be changed to background elements simultaneously. We use a brand–new approach; both *directional* and *subfield* methods are combined. The proof of topology preservation of the proposed algorithm is given in the Appendix.

Thinning Methodologies

In discrete spaces, only an approximation to the continuous skeleton can be produced. There are two major requirements to be complied with (Székely, 1996). The first one is *geometrical*. It means that the "skeleton" must be in the "middle" of the object and invariant under geometrical transformations. The second one is *topological* requiring that the "skeleton" must be topologically equivalent to the original object. The major aim of thinning is to reduce the object in a topology preserving way.

A 3D binary picture is a mapping that assigns value of 0 or 1 to each point with integer co-ordinates in the 3D digital space denoted by $\mathbb{Z}^3$. Points having the value of 1 are called black points, while 0's are called white ones. Black points form objects of the picture. White points form the background and the cavities of the picture. Both the input and the output of a picture operation are pictures. An operation is reduction if it can delete some black points (i.e., changes them to white) but white points remain the same. There is a fairly general agreement that a reduction operation is *not* topology preserving if any object in the input picture is split (into two or more ones) or completely deleted, if any cavity in the input picture is merged with the background or another hole, or if a cavity is created where there was none in the input picture (Kong, 1995). There is an additional concept called hole in 3D pictures. A hole (that doughnuts have) is formed by 0's, but it is not a cavity. Topology preservation implies that eliminating or creating any hole is not allowed. (Formal definitions of the concepts of digital topology and the criterion of topology preservations can be found in the Appendix.)

Existing 3D thinning algorithms can be classified from several points of view. One of them is the classification on the produced skeletons: most of the developed algorithms result in *medial surfaces* (Reed, 1984) and a few can produce *medial lines* (see Fig. 1). The aim of the thinning algorithms that are developed to extract medial lines is to shrink an object to one point width line segments.

Some algorithms have been developed for generating medial surface (Gong & Bertrand, 1990; Bertrand & Aktouf, 1994; Bertrand, 1995; Ma,

1995; Saha & Dutta Majumder, 1997), others allow producing medial surface and medial lines as well (Tsao & Fu, 1981; Lee et al., 1994; Bertrand & Aktouf, 1994) and there are some for extracting medial lines without creating medial surface as intermediate result (Ma & Sonka, 1996; Palágyi & Kuba, 1997).

Three types of parallel thinning methodologies have been proposed.

- The first type examines the $3 \times 3 \times 3$ neighbourhood of each border point. The iteration steps are divided into a number of subiterations. Only border points having the prescribed $3 \times 3 \times 3$ neighbourhood can be deleted during a subiteration. It means that each prescribed neighbourhood gives a deletion condition. Prescribed neighbourhoods can be usually associated to a direction (e.g., up, down) depending on the position of the border points to be deleted. These algorithms use *border sequential* or *directional* strategy. Each subiteration is executed in parallel (Tsao & Fu, 1981; Gong & Bertrand, 1990; Lee et al., 1994; Bertrand, 1995; Palágyi & Kuba, 1997) (i.e., all black points satisfying the deletion condition of the actual subiteration are simultaneously deleted). Most of the existing parallel thinning algorithms are border sequential. Generally, 6 subiterations are used (with the exception of Palágyi & Kuba (1997)).

A directional algorithm consisting of k subiterations can be sketched by the following program:

```
repeat
    for i = 1 to k do
        simultaneous deletion of the black
        points that satisfy the condition
        assigned to the i–th direction
until no points are deleted
```

- The second type of algorithms does not need subiterations. In order to preserve topology, the existing two *fully parallel* algorithms investigate some points that are in the $5 \times 5 \times 5$ neighbourhood but not in the $3 \times 3 \times 3$ neighbourhood (Ma, 1995; Ma & Sonka, 1996).

These algorithms can be sketched by the following program:

```
repeat
    simultaneous deletion of the black
    points that satisfy the global condition
until no points are deleted
```

- The third approach is the *subfield sequential method*. The set of points $\mathbb{Z}^3$ is subdivided into more disjoint subfileds which are alternatively activated. At a given iteration step, only black points of the active subfield are designated to be deleted.

A subfield based algorithm consisting of k subfields can be sketched by the following program:

```
repeat
    for i = 1 to k do
        simultaneous deletion of the black
        points in the i–th subfield
        that satisfy the global condition
        assigned to each subfield
until no points are deleted
```

Two subfield sequential 3D thinning algorithms working in cubic grid $\mathbb{Z}^3$ have been proposed so far (Bertrand & Aktouf, 1994; Saha & Dutta Majumder, 1997).

This paper presents an algorithm, which belongs to a brand–new class of thinning methods called *hybrid* algorithms. It applies both directional and subfield strategies. A hybrid algorithm containing k_1 directional subiterations and k_2 subfields is described by the following program:

```
repeat
    remark the k1 directional–type subiterations
        for i = 1 to k1 do
            simultaneous deletion of the black
            points that satisfy the condition
            assigned to the i–th direction
    remark the k2 subfield–type subiterations
        for j = 1 to k2 do
            simultaneous deletion of the black
            points in the j–th subfield that satisfy
            the global condition assigned to each
            subfield
until no points are deleted
```
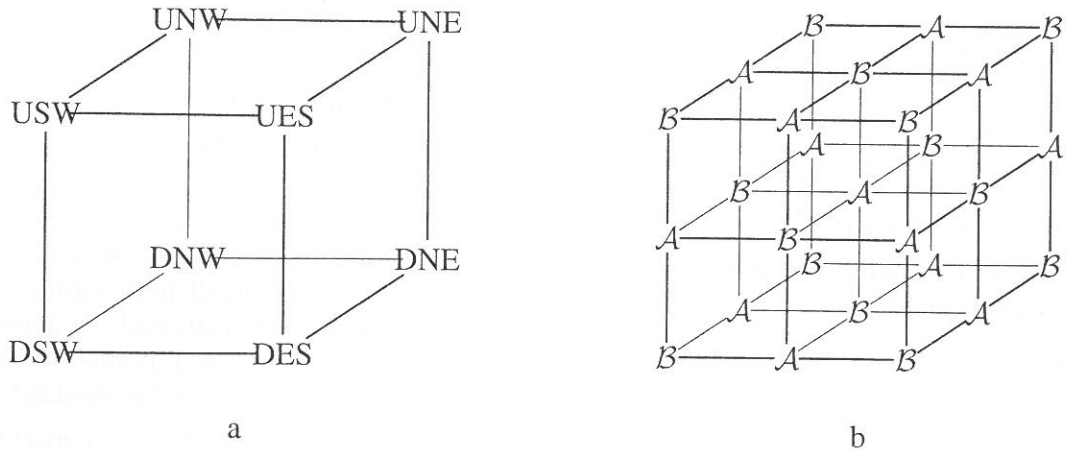
Fig. 2. The 8 deletion directions associated with the 8 vertices of a cube (a). These directions are denoted by USW,...,DNE. A 3D $3 \times 3 \times 3$ "chessboard–like" pattern determined by the two subfileds (b). Points in $\mathcal{SF}_A$ and $\mathcal{SF}_B$ are labelled by $\mathcal{A}$ and by $\mathcal{B}$, respectively.

The New Thinning Algorithm

In this section a hybrid 3D thinning algorithm is described that directly creates medial lines (i.e., without extracting medial surface as intermediate result).

One iteration step contains 8 directional–type subiterations (according to the selected 8 deletion directions) and 2 subfield–type subiterations (according to the 2 subfields). The 8 deletion directions are associated with the 8 vertices of a cube. These directions are denoted by USW, DNE, USE, DNW, UNE, DSW, UNW, and DSE, see Fig. 2 (a). Note that each directional 3D thinning algorithm uses the 6 deletion directions associated with the 6 faces of a cube (with the exception of Palágyi & Kuba (1997)). The set $\mathbb{Z}^3$ is subdivided into two disjoint subfields called $\mathcal{F}_A$ and $\mathcal{F}_B$. The pattern determined by the two subfields is presented in Fig. 2 (b). These two subfields are given by the following formulae:
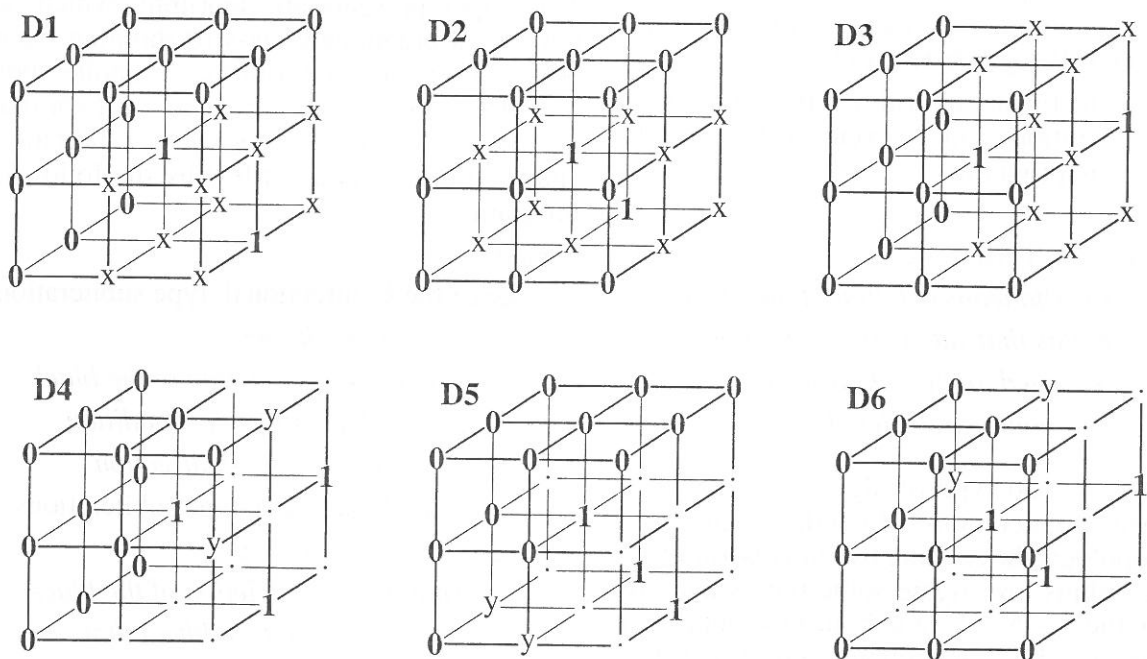

Fig. 3. Templates **D1**–**D6** form the set of templates $\mathcal{T}_{\text{USW}}$. (Note, that at least one point marked "x" is 1 (black) in each of the templates **D1**–**D3** and at least one point marked "y" is 0 (white) in each of the templates **D4**–**D6**.)

$$\mathcal{SF}_{\mathcal{A}} = \{ (x, y, z) \mid (x, y, z) \in \mathbb{Z}^3$$
$$\text{and } x + y + z \text{ is odd } \},$$
$$\mathcal{SF}_{\mathcal{B}} = \{ (x, y, z) \mid (x, y, z) \in \mathbb{Z}^3$$
$$\text{and } x + y + z \text{ is even } \}$$
$$= \mathbb{Z}^3 \backslash \mathcal{SF}_{\mathcal{A}},$$

Each iteration step contains 10 parallel subiterations. (8 successive directional–type subiterations are followed by 2 subfield–type ones.)

The new value of each voxel depends on its $3 \times 3 \times 3$ neighbourhood in each subiteration. This dependence is given by a set of configurations of $3 \times 3 \times 3$ lattice points called deletion templates. A black point is to be deleted if and only if its $3 \times 3 \times 3$ neighbourhood matches at least one element of the given set of templates. Templates usually contain three kinds of elements, 1 (black), 0 (white), and "." ("don't care"), where a "don't care" element matches either a black point or a white point in a given picture.

The set of templates $\mathcal{T}_{USW} = \{\mathbf{D1}, \ldots, \mathbf{D6}\}$ assigned to the deletion direction USW are given by Fig. 3. The other seven sets of templates assigned to the other seven directional–type subiterations can be derived from the appropriate rotations and reflections of the templates in $\mathcal{T}_{USW}$. It means that different deletion conditions are assigned to the 8 directional–type subiterations.

The two subfield–type subiterations have a common global deletion condition given by the set
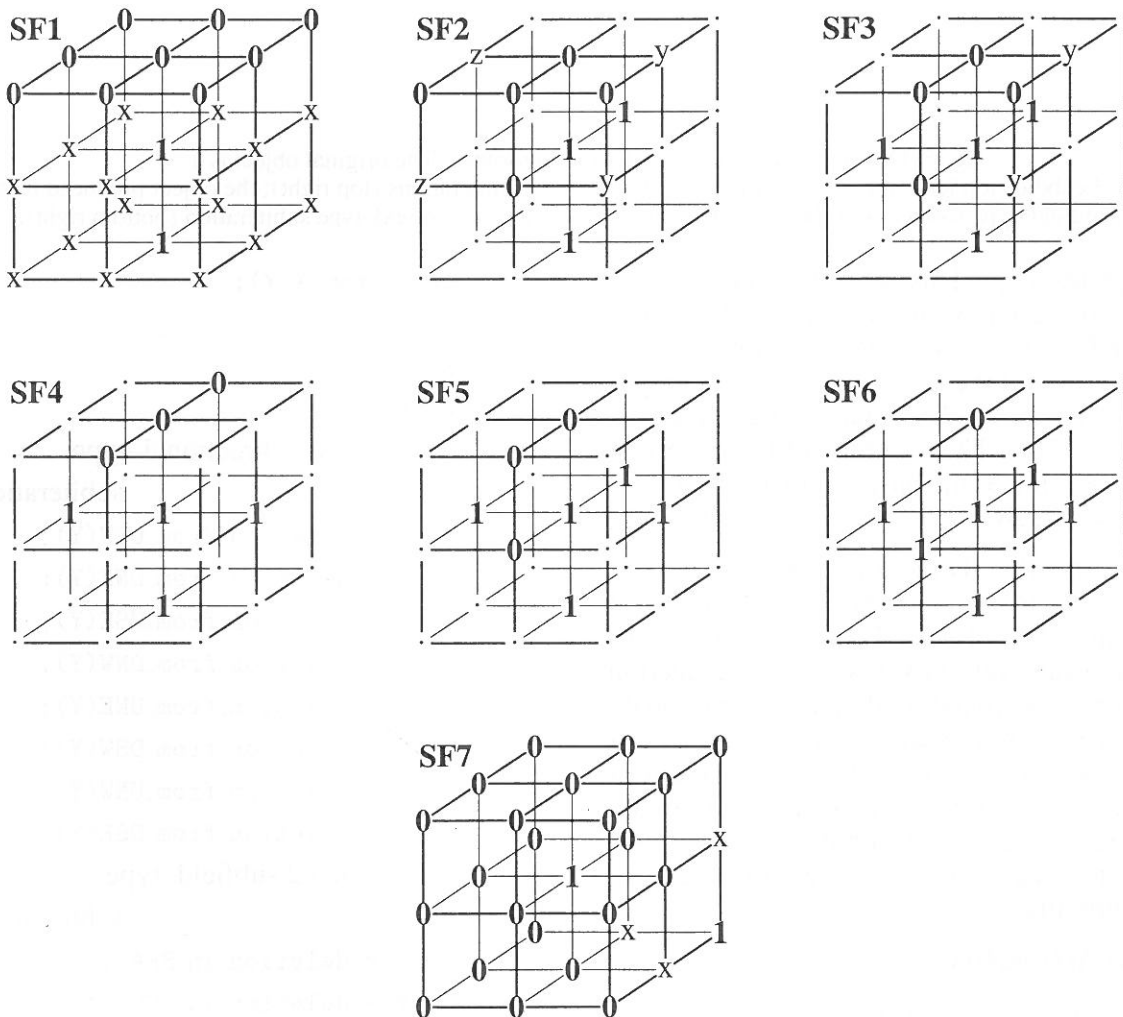

Fig. 4. Base templates **SF1**–**SF7** and their all rotations and reflections form the set of templates $\mathcal{T}_{\mathcal{SF}}$. (Note, that at least one point marked "x" is 1 (black) in each template **SF1** and **SF7**; at least one point marked "y" is 0 (white) in each template **SF2** and **SF3**; and at least one point marked "z" is 0 (white) in the template **SF2**.)
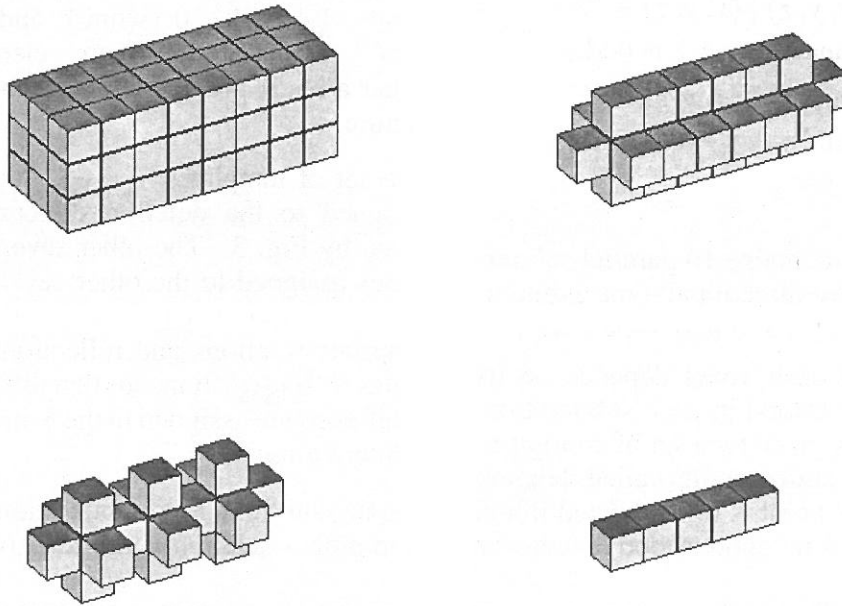
Fig. 5. One iteration step of the Hybrid Algorithm. The original object is a
$3 \times 8 \times 3$ cuboid (top left); the result of the 8 directional–type subiterations (top right); the object produced by the
1st subfield–type subiteration (bottom left); the result of the 2nd subfield–type subiteration (bottom right).

of templates $\mathcal{T}_{\mathcal{SF}}$. This set of templates is represented by seven, what is called base templates **SF1–SF7**, see Fig. 4. All reflections and all rotations around the axes of the base templates are templates, too. (The rotation angles are 90°, 180°, and 270°. The numbers of template versions belonging to the base templates **SF1**, . . . , **SF7** are 6, 12, 24, 12, 12, 6, and 8, respectively.)

Suppose that the 3D picture to be thinned contains finitely many black points. Therefore, it can be stored in a finite 3D binary array. (Outside this array every voxel is white.) Reduction operations associated with the 8 directional–type subiterations are called `deletion_from_USW`, ... , `deletion_from_DSE`. The two operations belonging to the subfield–type subiterations are called `deletion_in_SFA` and `deletion_in_SFB`. We are now ready to present the proposed algorithm formally.

HYBRID ALGORITHM:

Input: binary array X that represents
   the picture to be thinned
Output: binary array Y that represents
   the thinned picture

```
Hybrid_Algorithm(X,Y);
   begin
      Y=X;
      repeat
         remark the 8 directional-type
                              subiterations
            Y = deletion_from_USW(Y);
            Y = deletion_from_DNE(Y);
            Y = deletion_from_USE(Y);
            Y = deletion_from_DNW(Y);
            Y = deletion_from_UNE(Y);
            Y = deletion_from_DSW(Y);
            Y = deletion_from_UNW(Y);
            Y = deletion_from_DSE(Y);
         remark the 2 subfield-type
                              subiterations
            Y = deletion_in_SFA(Y);
            Y = deletion_in_SFB(Y);
      until no points are deleted;
   end.
```
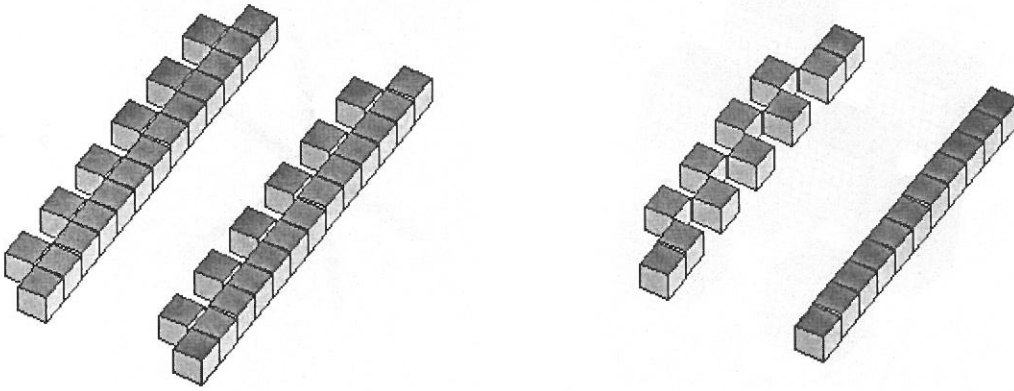
Fig. 6. Sensitivity of the Hybrid Algorithm to object position. Two objects of the same shape whose appropriate points are in different subfields (left) and their medial lines (right).
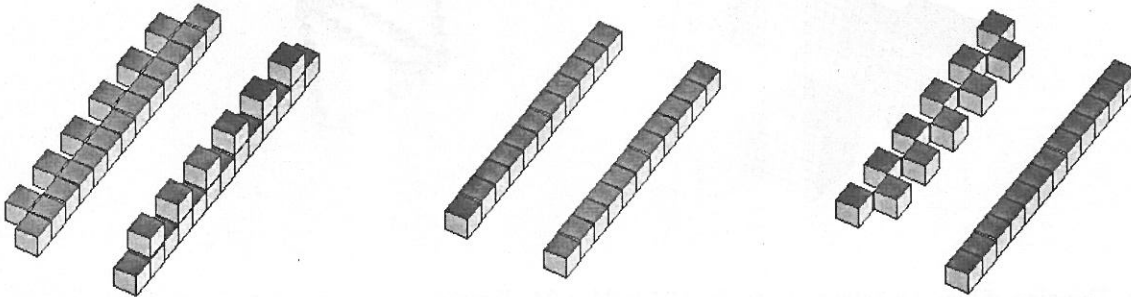

Fig. 7. Relative invariance under object rotation. Two objects of the same shape (left); their medial lines produced by Hybrid Algorithm (centre); medial lines extracted by a directional algorithm (Palágyi & Kuba, 1997) (right).

The steps of the Hybrid Algorithm are demonstrated in Fig. 5. The proposed algorithm terminates when there is no black point deleted by the last iteration step. Since all considered input pictures contain finitely many black points, it will terminate after a finitely many iteration steps.

Discussion

Thinning based skeleton extraction concentrates on the topological requirement. A thinning algorithm uses the distance induced by its object reduction strategy. This distance cannot be regarded as a good approximation to the Euclidean distance. Therefore, thinning algorithms are not invariant under geometrical transformations. Directional and fully parallel algorithms are able to produce invariant results under object translation. Unfortunately, it does not hold for subfield sequential algorithms. That is the reason why the Hybrid Algorithm is sensitive to the object position (see Fig. 6). On the other hand directional algorithms are more sensitive to object rotation (see Fig. 7).

The Hybrid Algorithm has been tested for several synthetic pictures. Here we present some examples. The results of thinning for four synthetic 3D objects can be seen in Figs. 8–9. Our algorithm creates nearly regular and symmetric medial lines from regular and symmetric objects. The Hybrid Algorithm was also tested for thinning 3D binary objects extracted from magnetic resonance angiographies (MRA studies). An example is shown in Fig. 10.

The skeleton represents local object symmetries (Blum, 1967). In 3D, skeletal surface points represent mirror symmetry and skeletal line points represent axial symmetry. Some of the general symmetry about an object can be found
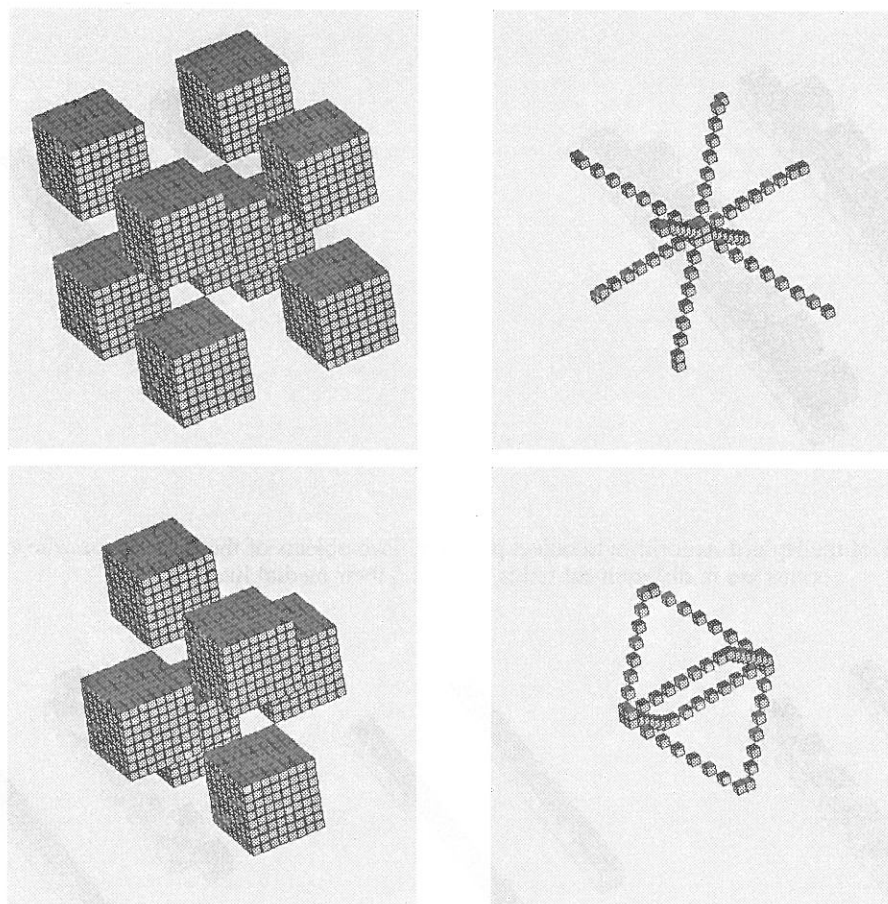
Fig. 8. Thinning of two synthetic pictures sized 24 × 24 × 24. The original objects (left) and their medial lines extracted by the Hybrid Algorithm (right).

in the skeleton but others are suppressed. Extracting medial lines is more relevant for some types of medical images than producing medial surface. These types of medical images contain blood vessels, bones or airway trees (after segmentation).

Most 3D thinning algorithms are capable of producing medial surface, therefore, those ones are not suggested to the objects listed above. Some authors (for example Tsao & Fu (1981)) have proposed a 2–phase process for medial lines thinning. After the first phase, each object in the original picture is reduced into its medial surface. After the second phase, each medial surface is converted into medial lines. It is shown in (Palágyi & Kuba, 1997) that the 2–phase method produces a lot of unwanted parasitic line segments. That is the reason why the Hybrid Algorithm directly extracts medial lines.

We give the deletable points of the Hybrid Algorithm by sets of templates (instead of checking windows (Tsao & Fu, 1981) or labelling procedure and Euler–table (Lee et al., 1994)). It is easy to see that each template can be replaced by a Boolean formula. Therefore, the Hybrid Algorithm makes easy implementation possible. It has been proved that the Hybrid Algorithm preserves topology. (Proofs can be found in the Appendix.)

Both of the published subfield sequential 3D thinning algorithms use 8 subfields (Bertrand & Aktouf, 1994; Saha & Dutta Majumder, 1997). It is not by accident, since the proof of topology preserving is trivial in that case. Our algorithm is an example to illustrate that it is possible to develop 2–subfield thinning algorithms with the help of other technique (e.g., directional thinning).
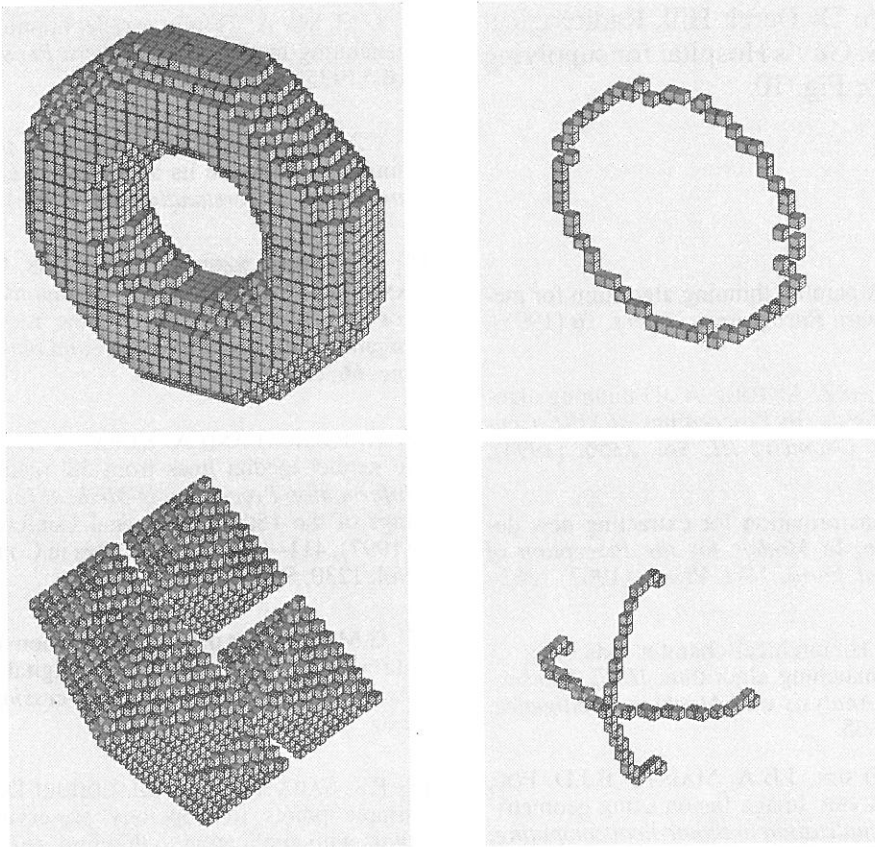
Fig. 9. Thinning of two synthetic pictures sized $40 \times 40 \times 20$. The original objects (left) and their medial lines extracted by the Hybrid Algorithm (right).
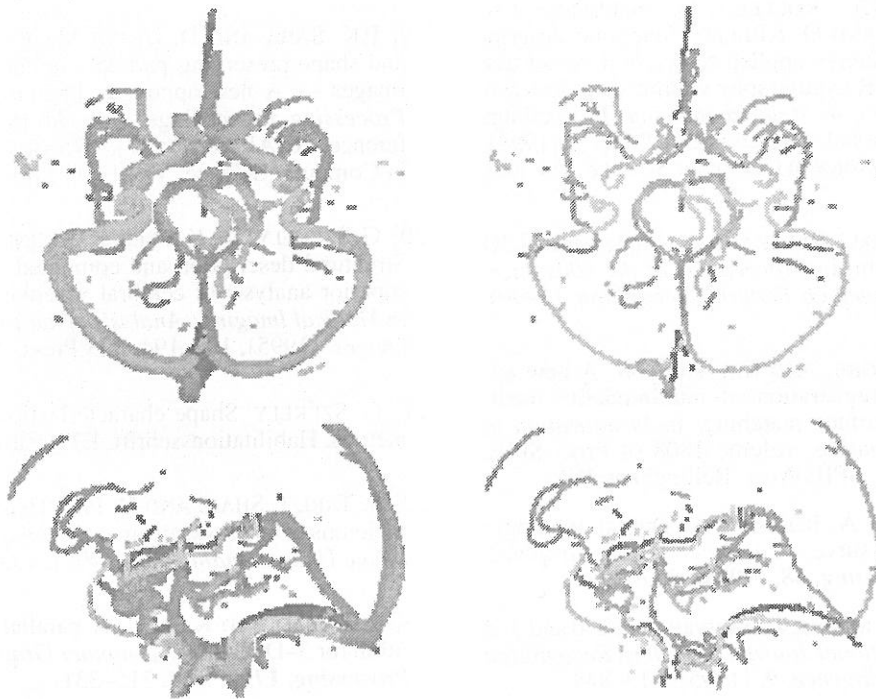

Fig. 10. Thinning of brain blood vessels by the Hybrid Algorithm. The binary objects were extracted from a (greyscale) 3D MRA study of dimensions $256 \times 256 \times 124$. The top–down projection of the original binary objects (top left) and their medial lines (top right). The left–right projection of the original binary objects (bottom left) and the medial lines extracted from them (bottom right). Projections of these pictures are displayed by using the 3DVIEWNIX software system (Udupa et al., 1994).

References

[1] G. BERTRAND A parallel thinning algorithm for medial surfaces. *Pattern Recognition Letters*, **16** (1995), 979–986.

[2] G. BERTRAND AND Z. AKTOUF A 3D thinning algorithms using subfields. In *Proceedings of SPIE Conference on Vision Geometry III*, Vol. 2356, (1994), 113–124.

[3] H. BLUM A transformation for extracting new descriptors of shape. In *Models for the Perception of Speech and Visual Form*, MIT Press, (1967), 362–380.

[4] G. BORGEFORS Hierarchical chamfer matching: A parametric edge matching algorithm. *IEEE Transactions on Pattern Analysis and Machine Intelligence*, **10**, (1988), 849–865.

[5] P.A. VAN DEN ELSEN, J.B.A. MAINTZ, E.J.D. POL, AND M.A. VIERGEVER Image fusion using geometrical features. In *Visualization in biomedical computing*, volume 1808 of Proc. SPIE, (1992), 172–186, SPIE Press, Bellingham, WA.

[6] G. GERIG, TH. KOLLER, G. SZÉKELY, CH. BRECHBÜHLER, AND O. KÜBLER Symbolic description of 3–D structures applied to cerebral vessel tree obtained from MR angiography volume data. In *Information Processing in Medical Imaging*, Proceedings of 13th International Conference, IPMI'93, (1993), 94–111, Lecture Notes in Computer Science, Vol. 687, Springer–Verlag.

[7] W.X. GONG AND G. BERTRAND A simple parallel 3D thinning algorithm. In *Proceedings of the 10th International Conference on Pattern Recognition*, (1990), 188–190.

[8] H. JIANG, A. ROBB, AND K.S. HOLTON A new approach to 3-D registration of multimodality medical images by surface matching. In *Visualization in biomedical computing*, volume 1808 of Proc. SPIE, 196–213, (1992), SPIE Press, Bellingham, WA.

[9] T.Y. KONG AND A. ROSENFELD Digital topology: Introduction and survey. *Computer Vision, Graphics, and Image Processing*, **48**, (1989), 357–393.

[10] T.Y. KONG On topology preservation in 2–d and 3–d thinning. *International Journal of Pattern Recognition and Artifical Intelligence*, **9**, (1995), 813–844.

[11] T. LEE, R.L. KASHYAP, AND C. CHU Building skeleton models via 3–D medial surface/axis thinning algorithms. *CVGIP: Graphical Models and Image Processing*, **56**, (1994), 462–478.

[12] C.M. MA On topology preservation in 3D thinning. *CVGIP: Image Understanding*, **59**, (1994), 328–339.

[13] C.M. MA A 3D fully parallel thinning algorithm for generating medial faces. *Pattern Recognition Letters*, **16**, (1995), 83–87.

[14] C.M. MA AND M. SONKA A fully parallel 3D thinning algorithm and its applications. *Computer Vision and Image Understanding*, **64**, (1996), 420–433.

[15] M. NÄF, G. SZÉKELY, R. KIKINIS, M.E. SHENTON, AND O. KÜBLER 3D Voronoi skeletons and their usage for the characterization and the recognition of 3D organ shape. *Computer Vision and Image Understanding*, **66**, (1997), 147–161.

[16] K. PALÁGYI AND A. KUBA A thinning algorithm to extract medial lines from 3D medical images. In *Information Processing in Medical Imaging*, Proceedings of the 15th International Conference, IPMI'97, (1997), 411–416, Lecture Notes in Computer Science, Vol. 1230, Springer.

[17] G.M. REED On the characterization of simple closed surfaces in three–dimensional digital images. *Computer Graphics and Image Processing*, **25**, (1984), 226–235.

[18] P.K. SAHA AND B.B. CHAUDHURI Detection of 3–D simple points for topology preserving transformations with application to thinning. *IEEE Transactions on Pattern Analysis and Machine Intelligence*, **16**, (1994), 1028–1032.

[19] P.K. SAHA AND D. DUTTA MAJUMDER Topology and shape preserving parallel thinning for 3D digital images — A new approach. In *Image Analysis and Processing*, Proceedings of the 9th International Conference, ICIAP'97, (1997), 575–581, Lecture Notes in Computer Science, Vol. 1310, Springer.

[20] G. SZÉKELY, TH. KOLLER, R. KIKINIS, AND G. GERIG Structural description and combined 3–D display for superior analysis of cerebral vascularity from MRA. In *Medical Imaging: Analysis of multimodality 2D/3D images*, (1995), 183–194, IOS Press, Amsterdam.

[21] G. SZÉKELY Shape characterization by local symmetries. Habilitationsschrift, ETH Zürich, 1996.

[22] S. TARI, J. SHAH, AND H. PIEN Extraction of shape skeletons from grayscale images. *Computer Vision and Image Understanding*, **66**, (1997), 133–146.

[23] Y.F. TSAO AND K.S. FU A parallel thinning algorithm for 3–D pictures. *Computer Graphics and Image Processing*, **17**, (1981), 315–331.

[24] J.K. UDUPA, D. ODHNER, S. SAMARASEKERA, R. GONCALVES, K. IYER, K. VENUGOPAL, AND S. FURUIE 3DVIEWNIX: An open, transportable, multidimensional, multimodality, multiparametric imaging software system. In *SPIE Proceedings*, Vol. 2164, (1994), 58–73.

Appendix

In this section, we prove that the Hybrid Algorithm preserves topology. At first some concepts of the digital topology and the applied results are presented.

The set $\mathbb{Z}^3$ is a *3D digital space* that contains points with integer coordinates. The three most important adjacency relations in $\mathbb{Z}^3$ are the 6–, the 18–, and the 26–*adjacency*. The set of points that are *j–adjacent* to a point p is denoted by $N_j(p)$, for $j = 6, 18, 26$ (see Fig. 11). The point p is said to be *j–adjacent* to the non–empty set of points X if there exists a point $x \in X$ so that $x \in N_j(p)$. The sequence of distinct points $\langle x_0, x_1, \ldots, x_n \rangle$ is a *j–path* of length $n \geq 0$ from point x_0 to point x_n in a non–empty set of points X if each point of the sequence is in X and x_i is *j–adjacent* to x_{i-1} for each $1 \leq i \leq n$. (Note that a single point is a *j–path* of length 0.) Two points are *j–connected* in the set X if there exists a *j–path* in X between them. A set of points X is *j–connected* if any two points in X are *j–connected* in X.
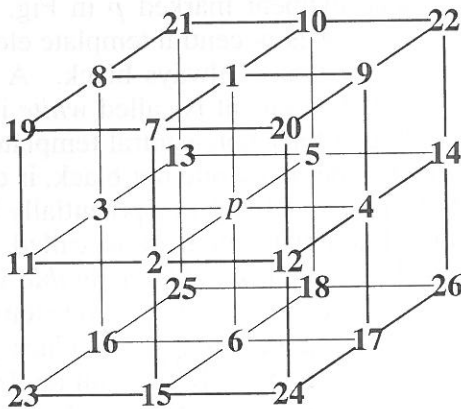
Fig. 11. The frequently used adjacencies in $\mathbb{Z}^3$. Points in $N_6(p)$ are marked **1–6**; points in $N_{18}(p)$ are marked **1–18**; points in $N_{26}(p)$ are marked **1–26**. (Note, that point p is in sets $N_6(p)$, $N_{18}(p)$, and $N_{26}(p)$.)

The *3D binary (m,n) digital picture* $\mathcal{P}$ is a quadruple $\mathcal{P} = (\mathbb{Z}^3, m, n, B)$ (Kong & Rosenfeld, 1989). A point in $B \subseteq \mathbb{Z}^3$ is called *black point*; a point in $\mathbb{Z}^3 \setminus B$ is called *white point*. Picture $\mathcal{P}$ is called *finite* if B is a finite set. Value of 1 is assigned to each black point and value

of 0 is assigned to each white point. m and n are two adjacency relations for black points and white points, respectively. Picture $\mathcal{P}$ is referred to as (m, n) picture, shortly. To avoid connectivity paradoxes, different adjacencies are treated. Most thinning algorithms deal with $(26, 6)$ pictures. Equivalence classes of B under m–connectivity are called *black m–components* or *objects*. Equivalence classes of $\mathbb{Z}^3 \setminus B$ under n–connectivity are called *white n–components*. In a finite picture there is a unique infinite white component, it is the *background*. A finite white component is called *cavity* in a 3D picture.

Iterative thinning algorithms delete black points that satisfy certain conditions. The entire process is repeated until there are no more black points to be changed. Each thinning algorithm should satisfy the requirement of topology preservation. We prove that the Hybrid Algorithm is topology preserving for any $(26, 6)$ pictures. Our proofs include the following results:

A black point is called *simple point* if its deletion does not alter the topology of the picture. We make use of the following criteria for $(26, 6)$ pictures:

THEOREM 1 (Saha & Chaudhuri, 1994). Black point p is simple in picture $\mathcal{P} = (\mathbb{Z}^3, 26, 6, B)$ if and only if all of the following three conditions hold:

1. The set $(B \setminus \{p\}) \cap N_{26}(p)$ contains exactly one 26–component.
2. The set $(\mathbb{Z}^3 \setminus B) \cap N_6(p)$ is not empty.
3. Any two points in $(\mathbb{Z}^3 \setminus B) \cap N_6(p)$ are 6–connected in the set $(\mathbb{Z}^3 \setminus B) \cap N_{18}(p)$.

According to Theorem 1 simplicity can be decided locally by examining the $3 \times 3 \times 3$ neighbourhood of black points.

Parallel reduction operations delete a set of black points and not only a single simple point. We need to consider what is meant under topology preservation when a number of black points are deleted simultaneously.

DEFINITION 2 (Ma, 1994). Let $\mathcal{P}$ be a picture. The set $D = \{d_1, \ldots, d_k\}$ of black points is called *simple set* of $\mathcal{P}$ if D can be arranged

in a sequence $\langle d_{i_1}, \ldots, d_{i_k} \rangle$ in which each d_{i_j} is simple after $\{d_{i_1}, \ldots, d_{i_{j-1}}\}$ is deleted from $\mathcal{P}$, for $j = 1, \ldots, k$. (By definition, let the empty set be simple.)

This definition implies the next one.

DEFINITION 3 (Ma, 1994). A 3D parallel reduction operation is *topology preserving* if, for all possible 3D pictures, the set of all points that the operation simultaneously deletes is simple.

Fortunately, we do not have to test the algorithms for all possible 3D pictures. We only need to check a rather small number of configurations to prove topology preserving. Let a *unit lattice square* be a configuration of points of size $1 \times 2 \times 2$, $2 \times 1 \times 2$, or $2 \times 2 \times 1$. The configuration of $2 \times 2 \times 2$ points of $\mathbb{Z}^3$ is called a *unit lattice cube*.

THEOREM 4 (Ma, 1994). A 3D parallel reduction operation preserves topology for (26,6) pictures if all of the following conditions hold:

1. Only simple points can be deleted.
2. If two black corners, p and q, of a unit lattice square are deleted, then the set $\{p, q\}$ is simple.
3. If three black corners, p, q, and r, of a unit lattice square are deleted, then the set $\{p, q, r\}$ is simple.
4. If four black corners, p, q, r, and s, of a unit lattice square are deleted, then the set $\{p, q, r, s\}$ is simple.
5. No black component contained in a unit lattice cube can be deleted completely.

Instead of proving the conditions of Theorem 4, we use the following more general conditions:

THEOREM 5. Let $\mathcal{T}$ be a parallel reduction operation. Let p be any black point in any picture $\mathcal{P} = (\mathbb{Z}^3, 26, 6, B)$ so that p is deleted by $\mathcal{T}$. Let Q be any set of black points so that $Q \subseteq (N_{18}(p) \setminus \{p\}) \cap B$ in picture $\mathcal{P}$ and each point is Q is deleted by $\mathcal{T}$. Operation $\mathcal{T}$ preserves topology for (26,6) pictures if all of the following conditions hold:

1. p is simple in the picture $(\mathbb{Z}^3, 26, 6, B \setminus Q)$.

2. No black component contained in a unit lattice cube can be deleted completely by operation $\mathcal{T}$.

It is easy to see that Condition 1 of Theorem 5 implies Conditions 1–4 of Theorem 4, and Condition 2 of Theorem 5 corresponds to Condition 5 of Theorem 4. (It is obvious that the set $N_{18}(p)$ contains any unit lattice squares in which p is a corner. Point p is to be regarded as the last element of the simple sequence of corners while the preceding ones are in set Q. If $Q = \emptyset$, then we get Condition 1 of Theorem 4.)

We will prove that the directional–type subiteration corresponding to the direction USW and the first subfield–type subiteration (as parallel reduction operations) are both topology preserving.

In order to prove both conditions of Theorem 5, we classify the elements of templates and state some properties of the sets of templates $\mathcal{T}_{\text{USW}}$ and $\mathcal{T}_{\mathcal{SF}}$.

The template element marked p in Fig. 11 is called *central*. A non–central template element is called *black* if it is always black. A non–central template element is called *white* if it is always white. Other non–central template element which is neither white nor black, is called *potentially black*. A black or a potentially black non–central template element is called *non–white*. A black point is *USW–deletable* if and only if it can be deleted by at least one template in the set of templates $\mathcal{T}_{\text{USW}}$. A black point is *SF–deletable* if and only if it can be deleted by at least one template in the set of templates $\mathcal{T}_{\mathcal{SF}}$.

Let us state some properties of the set of templates $\mathcal{T}_{\text{USW}}$ (see Figs. 3 and 11).

OBSERVATION 6. For each template in $\mathcal{T}_{\text{USW}}$, each index in the set $\{7, 8, 11\}$ corresponds to a white template element.

OBSERVATION 7. For each template in $\mathcal{T}_{\text{USW}}$, the index corresponding to any template element is in the set $\{14, 17, 18\}$. (In other words, each black template element is 18–adjacent (but not 6–adjacent) to the central element.)
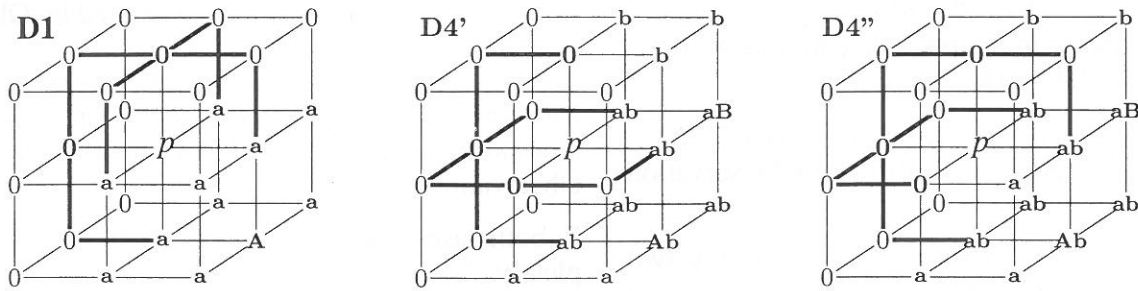
Fig. 12. Labels assigned to the non–white elements of the base templates **D1** and **DM4**. Template **D4** is decomposed into two ones denoted by **D4'** and **D4''**. Thick lines represent the required 6–paths in $(\mathbb{Z}^3 \backslash B) \cap N_{18}(p)$.

OBSERVATION 8. If a black point p can be deleted by a template in $\mathcal{T}_{USW}$ and the black point q coincides with a black element of that template, then point q is not USW–deletable. (It is implied by Observations 6 and 7.)

OBSERVATION 9. For each template in $\mathcal{T}_{USW}$, at least one index in the set $\{1, 2, 3\}$ corresponds to a white element. (In other words, each template contains at least one white element 6–adjacent to the central template element.)

We are ready to prove that the directional–type subiteration corresponding to the direction USW is topology preserving. The following two lemmas correspond to the two conditions of Theorem 5.

LEMMA 10. The first directional–type subiteration of the Hybrid Algorithm satisfies Condition 1 of Theorem 5.

PROOF. Let p be a USW–deletable point in a $(\mathbb{Z}^3, 26, 6, B)$ picture and let Q be a set of USW–deletable points so that $Q \subseteq (N_{18}(p) \backslash \{p\}) \cap B$. It is to be shown that p is simple after the deletion of Q.

We distinguish the following two cases:

(a) $Q = \emptyset$.
(b) $Q \neq \emptyset$.

In case (a), we have to prove that p is simple. We show that all of the conditions of Theorem 1 are satisfied.

The set of template $\mathcal{T}_{USW}$ contains the six templates **D1**–**D6**. It is easy to see that **D2** and **D3** can be derived from **D1** by arbitrary chosen rotations and reflections. Similarly, **D5** and **D6**

can be derived from **D4**. Simplicity is invariant under those kinds of transformations, therefore, we deal only with the two base templates **D1** and **D4**. Let us suppose that point p can be deleted by **D1** or **D4**.

Condition 1 of Theorem 1 says that $(B \backslash \{p\}) \cap N_{26}(p)$ must contain exactly one 26–component. It is shown with the help of Fig. 12. Labels **A** and **B** are assigned to the black template elements. Labels **a** and **b** are assigned to non–white elements 26–adjacent to the black element labelled by **A** and **B**, respectively. Obviously, a point may be 26–adjacent to more certainly black points. In this case, it is multiply labelled. We show that there exists a 26–path containing only non–white positions between any two non–white points.

The only black element in base template **D1** is labelled by **A**. We can state that all potentially black points are labelled by **a** in these templates. It is easy to see that any two non–white points are 26–connected via an at most two–length 26–path. The sequence of labels in this path can be $\langle \mathbf{a}, \mathbf{A} \rangle$ or $\langle \mathbf{a}, \mathbf{A}, \mathbf{a} \rangle$.

Base template **D4** contains two black elements labelled by **Ab** and **aB**, respectively. All potentially black elements are labelled in these templates, too. It is easy to see that any two non–white points are 26–connected via an at most three–length 26–path. The sequence of labels in this path can be

$\langle \mathbf{a?}, \mathbf{Ab}, \mathbf{a?} \rangle$,
$\langle \mathbf{a?}, \mathbf{Ab}, \mathbf{aB}, \mathbf{?b} \rangle$, or
$\langle \mathbf{?b}, \mathbf{aB}, \mathbf{?b} \rangle$,

where "?" can be replaced by the appropriate characters **a**, **b**, or the empty string. Note that any prefix of a path is a path, too.

We can state that $(B \setminus \{p\}) \cap N_{26}(p)$ contains exactly one (non–empty) 26–component if p is deleted by **D1** or **D4**.

Condition 2 of Theorem 1 (i.e., set $(\mathbb{Z}^3 \setminus B) \cap N_6(p)$ is not empty) is fulfilled by Observation 9.

Condition 3 of Theorem 1 says that any two points in $(\mathbb{Z}^3 \setminus B) \cap N_6(p)$ must be 6–connected in the set $(\mathbb{Z}^3 \setminus B) \cap N_{18}(p)$. It is shown with the help of Fig. 12, too. The required 6–paths are marked thick lines.

It has been shown that any USW–deletable point is simple.

Let us deal with the case **(b)**.

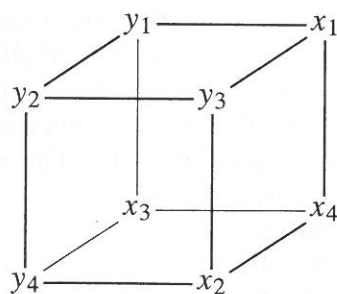It is to be shown that p is simple after the deletion of Q, where $Q \neq \emptyset$.

There is no black template element that coincides with any point in Q by Observation 8. Therefore, each point in Q must coincide with a potentially black template position. Simplicity of p does not depend on the potentially black template positions (see the proof of case **(a)**). $\square$

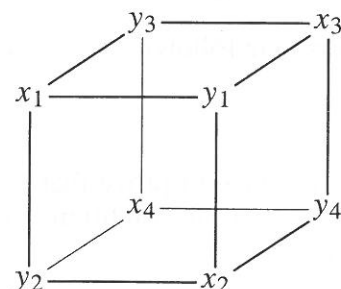LEMMA 11. The first directional–type subiteration of the Hybrid Algorithm satisfies Condition 2 of Theorem 5.

PROOF. Let us suppose that the two sets of points $X = \{x_1, x_2, x_3, x_4\}$ and $Y = \{y_1, y_2, y_3, y_4\}$ form a unit lattice cube in a picture as it is illustrated in Fig. 13 (a). Let C be an object contained in this unit lattice cube.

Two cases are to be distinguished:
(a) $C \cap X \neq \emptyset$
(b) $C \cap X = \emptyset$

In case (a), no point in X can be deleted by Observation 7.
In case (b), $C \cap Y \neq \emptyset$, since object C contains at least one point. Let us suppose that there exists a point in Y that can be deleted. It contradicts Observation 8, since $C \cap X = \emptyset$.

In both cases, object C cannot be deleted completely. $\square$

It has been proved that the subiteration associated with the deletion direction USW satisfies both conditions of Theorem 5, therefore, it is topology preserving. Let us deal with the first subfield–type subiteration. Some properties of the set of templates $\mathcal{T}_{\mathcal{SF}}$ and the applied subfield subdivision are to be stated (see Figs. 2 (b), 4, and 11).

OBSERVATION 12. Let p be a SF–deletable point in a picture. Then any black point $q \in (N_{26}(p) \setminus N_{18}(p)) \cup (N_6(p) \setminus \{p\})$ is not SF–deletable (because q is in the opposite subfield that is not active when p can be deleted).

OBSERVATION 13. For each template in the set of templates $\mathcal{T}_{\mathcal{SF}}$, the index of each black element is in $\{1, \ldots, 6, 19, \ldots, 26\}$.

OBSERVATION 14. If a black point p can be deleted by a template in $\mathcal{T}_{\mathcal{SF}}$ and the black point q coincides with a black element of that template, then point q is not SF–deletable. (It is implied by Observations 12 and 13.)

OBSERVATION 15. Each template in $\mathcal{T}_{\mathcal{SF}}$ contains at least one white element 6–adjacent to the central template element.

a   b

Fig. 13. Two unit lattice cubes formed by the sets of points $X = \{x_1, x_2, x_3, x_4\}$ and $Y = \{y_1, y_2, y_3, y_4\}$.

We are ready to prove that the first subfield–type subiteration is topology preserving. The following two Lemmas correspond to the two conditions of Theorem 5.

LEMMA 16. The first subfield–type subiteration of the Hybrid Algorithm satisfies Condition 1 of Theorem 5.

PROOF. Let p be a SF–deletable point in a $(\mathbb{Z}^3, 26, 6, B)$ picture and let Q be a set of SF–deletable points so that $Q \subseteq (N_{18}(p) \setminus \{p\}) \cap B$. It is to be shown that p is simple after the deletion of Q.

We distinguish the following two cases:

(a) $Q = \emptyset$.
(b) $Q \neq \emptyset$.

In case (a), we have to prove that p is simple. We show that all of the conditions of Theorem 1 are satisfied.

For the sake of brevity, only a sketch is given.

Condition 1 of Theorem 1 is fulfilled if p is 26–adjacent to only one 26–component of $N_{26}(p) \cap (B \setminus \{p\})$. It can be carried out as it was shown in the proof of Lemma 10. The same labelling procedure can be applied for each template in $\mathcal{T}_{\mathcal{SF}}$. Each non–white point can be labelled and any two non–white points can be connected via a n–length 26–path $\langle p_0, \ldots, p_n \rangle$, where p_i is a black template element, for each $1 \leq i \leq (n-1)$, and $n \geq 2$ if both p_0 and p_n correspond to potentially black template elements.

Condition 2 of Theorem 1 (i.e., set $(\mathbb{Z}^3 \setminus B) \cap N_6(p)$ is not empty) is fulfilled by Observation 15.

Condition 3 of Theorem 1 says that any two points in $(\mathbb{Z}^3 \setminus B) \cap N_6(p)$ must be 6–connected in the set $(\mathbb{Z}^3 \setminus B) \cap N_{18}(p)$. It can be proved as it was done in the proof of Lemma 10.

It can be carried out that any SF–deletable point is simple and its simplicity does not depend on potentially black template elements.

Let us deal with the case (b).

It is to be shown that p is simple after the deletion of Q, where $Q \neq \emptyset$.

There is no black template element that coincides with any point in Q by Observation 14. Therefore, each point in Q must coincide with a potentially black template position. Simplicity of p does not depend on the potentially black template positions (as it was stated in the sketch of the proof of case (a)). □

LEMMA 17. The first subfield–type subiteration of the Hybrid Algorithm satisfies Condition 2 of Theorem 5.

PROOF. Let us suppose that the two sets of points $X = \{x_1, x_2, x_3, x_4\}$ and $Y = \{y_1, y_2, y_3, y_4\}$ form a unit lattice cube in a picture as it is illustrated in Fig. 13 (b). We can state that sets X and Y are in opposite subfields. Let C be an object contained in this unit lattice cube. We know that black points in subfield $\mathcal{SF}_A$ are meant to be deleted during the first subfield–type subiteration.

Two cases are to be distinguished:

(a) $X \subset \mathcal{SF}_A$, and $Y \subset \mathcal{SF}_B$,
(b) $Y \subset \mathcal{SF}_A$, and $X \subset \mathcal{SF}_B$.

We will deal with only the case (a). The case (b) can be carried out analogously.

Case (a) is divided into the following two subcases:

(aa) $C \cap X = \emptyset$,
(ab) $C \cap X \neq \emptyset$.

In case (aa), $C \cap Y = Y \neq \emptyset$, since object C contains at least one point. No point in Y is SF–deletable, since $Y \subset \mathcal{SF}_B$. Therefore, object C cannot be deleted completely. As far as (ab) is concerned, we distinguish two additional cases:

(aba) there is a point in $C \cap X$ so that it is not SF–deletable.
(abb) for each point in $C \cap X$ is SF–deletable.

In case (aba), there is no problem. In case (abb), $C \cap Y \neq \emptyset$ by Observation 13. No point in Y is SF–deletable, since $Y \subset \mathcal{SF}_B$. Therefore, object C cannot be deleted completely either. □

We are ready to state the main theorem.

THEOREM 18. The Hybrid Algorithm is topology preserving.

PROOF. The first directional–type subiteration (associated with the deletion direction USW) is topology preserving by Lemmas 10 and 11. It can be proved for the other seven directional–type subiterations in a similar way.

The first subfield–type subiteration is topology preserving by Lemmas 16 and 17. This property can be proved for the second subfield–type subiteration in a similar way.

It is obvious that a complex operation consisting of a sequence of topology preserving operations is topology preserving, too. Therefore, the entire Hybrid Algorithm is topology preserving. □

We managed to prove that the Hybrid Algorithm is topology preserving. New conditions have been given for topology preservation that make relatively short proofs possible. We hope that Theorem 5 — that contains less and more general conditions than Theorem 4 — will be useful for other algorithms, too.

Contact address:
Kálmán Palágyi and Attila Kuba
Department of Applied Informatics
József Attila University
H-6701 Szeged P.O.Box 652
phone: 36 62 311184
fax: 36 62 312292
Hungary
e-mail: `palagyi@inf.u-szeged.hu`

e-mail: `kuba@inf.u-szeged.hu`

KÁLMÁN PALÁGYI has recently become assistant professor at the Department of Applied Informatics, József Attila University, Szeged. His research interests include medical image registration, fusion and 3D parallel thinning algorithms.

ATTILA KUBA is the head of the Department of Applied Informatics, József Attila University, Szeged. His research interests are image processing, its applications in medicine, image reconstruction and discrete tomography.